Sensitive label-free and compact biosensor based on concentric silicon-on-insulator microring resonators

Xiaohui Li,[1] Ziyang Zhang,[2] Shenying Qin,[3] Tao Wang,[1] Fangfei Liu,[1] Min Qiu,[2] and Yikai Su[1,*]

[1]Department of Electronic Engineering, Shanghai Jiao Tong University, Shanghai 200240, China

[2]Department of Microelectronics and Applied Physics, Royal Institute of Technology (KTH), Electrum 229, 164 40 Kista, Sweden

[3]Bio-X Life Science Research Center, Shanghai Jiao Tong University, Hao Ran Building, Shanghai 200030, China

*Corresponding author: yikaisu@sjtu.edu.cn

Received 2 February 2009; revised 12 June 2009; accepted 5 July 2009; posted 10 July 2009 (Doc. ID 107058); published 21 July 2009

We propose an ultracompact parallel label-free biosensor based on concentric silicon-on-insulator microring resonators. Our numerical studies show that the proposed biosensor offers higher sensitivity and a larger detection area than conventional single-ring-based sensors. We analyze the detection sensitivity of the DNA hybridization by immobilizing the probe on top of the double concentric ring resonators and in the ring–ring air gap. For a concentric double-ring system with an area of 27.646 μm^2, the bulk detection sensitivity is 683 nm RIU^{-1}. The sensitive uniformity of the system related to the optical field distribution is also studied.

OCIS codes: 130.6010, 230.4555.

1. Introduction

Molecular detection is an important step in many applications, such as monitoring molecular reaction dynamics, measuring the quantitative concentration of a solution, and determining the affinity contacts for medical study and clinical diagnosis. Several kinds of biosensing platform have been proposed based on potentiometric, amperometric, magnetic, or optical transducers [1]. An optical transducer-based biosensor consists of three key components, i.e., an optical device, a molecular coating, and a microfluid channel. The optical device is the essential tool because the change of its optical property manifests the status of the biobody. Chemical modification via a suitable biointerface is needed to induce the optical change. Microfluid architecture is typically employed to control the flow and detect each unit independently.

Currently, commercial detection microarrays rely mainly on the labeled molecular detection method, which employs fluorescence or radioisotope techniques to transfer information about molecules. However, the labeling step is not only expensive but also complicates the sample preparation and detection process. Several approaches for direct detection have been reported, such as a surface plasma resonator [2], interferometers [3], and optical fiber sensors [4,5]. However, these sensors are usually large in size and difficult to construct. Ring resonators based on silicon nitride [6], polymer [7], and silicon-on-insulator (SOI) devices [8] have been demonstrated for label-free biosensing. Ring resonator-based sensors are more compact and have the potential of offering high sensitivity with a high quality Q factor.

0003-6935/09/250F90-05$15.00/0

In addition, SOI microring resonators are compatible with complementary metal oxide semiconductor fabrication technology, making them suitable for ultracompact and highly integrated photonic circuits. In most cases, a high Q factor and large extinction ratio are desired. Previous work focused on a single-ring structure. To the best of our knowledge, biosensors based on concentric ring resonators have not been studied. Here we analyze their transmission property and detection sensitivity and show that concentric ring resonators based on SOI technology are compact and can provide sensitive detection, with an enhanced resonance notch depth and enlarged field distribution.

2. Optical Device Physics

Figure 1 is a schematic of a single detection unit. We define the amplitude of the resonant mode in the outer and inner rings as $a(t)$ and $b(t)$, respectively. The input amplitude is S_i and the output amplitude is S_o. The coefficients for waveguide–ring coupling and ring–ring mutual coupling are denoted as κ and u, respectively. The transfer function can be expressed by [9–12]

$$T(\omega)=\frac{|S_o|^2}{|S_i|^2}=\left|1-\frac{|k_a^2|\left[j(\omega-\omega_b)+\frac{1}{\tau_b}\right]}{\left[j(\omega-\omega_a)+\frac{1}{\tau_a}\right]\left[j(\omega-\omega_b)+\frac{1}{\tau_b}\right]+u^2}\right|^2, \tag{1}$$

where ω_a and ω_b are the resonant frequencies in the outer and inner rings, respectively; and τ is the photon lifetime. $1/\tau=1/\tau_e+1/\tau_i$, where $1/\tau_e$ is the waveguide decay rate and $1/\tau_i$ is the decay rate that is due to intrinsic loss. The quality factor (Q) is determined by the photon lifetime, i.e., $Q=\omega_0\tau/2$. The waveguide–ring coupling coefficient and the power decay rate are related by $|\kappa|^2=2/\tau_e$. To simplify the analysis, we only consider the case when the two rings happen to resonate at the same frequency, which can be realized by fine tuning the free-spectral range (FSR) of the individual rings. For a complete drop, the mutual coupling coefficient must satisfy

$$u_m^2=\left(\frac{1}{\tau_{ae}}-\frac{1}{\tau_{ai}}\right)\frac{1}{\tau_b}=\frac{\omega_0^2}{4Q_b}\left(\frac{1}{Q_{ae}}-\frac{1}{Q_{ai}}\right). \tag{2}$$

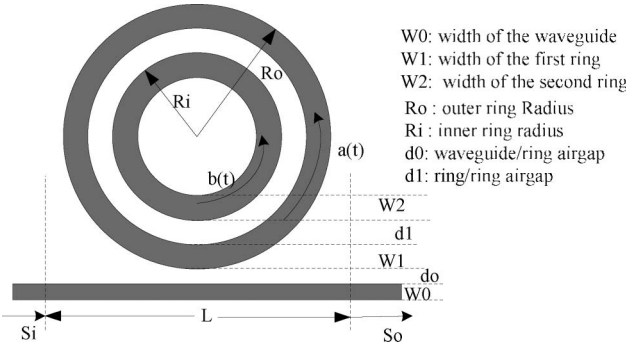

Fig. 1. Schematic of double concentric ring resonators and a waveguide coupled system.

We use two-dimensional (2D) finite-difference time-domain (FDTD) simulation [F2P, developed at the Royal Institute of Technology (KTH), Sweden] for our numerical studies. The simulation results show that the notch depths are much enhanced in the double concentric ring resonators compared with the single ring resonator [12]. To demonstrate the notch depth enhancement, we fabricated the device on a commercial SOI device. The measurement results in [11] confirm the notch depth enhancement by mutual coupling of the concentric rings. When the air gap between the straight waveguide and the ring resonator is small, for example, $0.11\,\mu$m as in the experiment, the coupling loss is larger than the intrinsic loss, resulting in a shallow notch depth that is due to overcoupling for a single-ring–single-waveguide system. For concentric ring resonators, mutual coupling helps the system to increase the effective intrinsic loss close to the coupling loss, making it easier for the system to reach critical coupling. Thus, it introduces another option to reach a critical coupling condition.

3. Biosensing with the Proposed Device

We use concentric ring resonators to detect the DNA hybridization. The effective refractive index of the waveguide changes after DNA hybridization, i.e., single-strand DNA (ssDNA) becomes double-strand DNA (dsDNA), leading to a resonance shift of the resonator system [13]. The refractive-index sensitivity of the detection system is defined as $d\lambda dn$, where λ is the resonance wavelength and n is the refractive index. The refractive indices of ssDNA and dsDNA layers are around 1.456 and 1.53, respectively, with a binding density of $1.49\,\text{pmol/cm}^2$ [14,15]. To model this, we apply the beam propagation method (BPM) from the commercial package offered by the Rsoft Design Group (Ossining, New York) and perform 2D FDTD simulations to study the detection performance of the resonator-based sensor system under different conditions.

A. Detection on Top of the Ring Resonators

We assume that the ssDNA is initially immobilized on the functionalized silicon layer in concentric ring resonators as the probe. First, we employ the BPM to simulate the electrical field profile of the multilayer structure before and after DNA hybridization. Figure 2(a) illustrates the multilayer structure that consists of a top biomolecular layer of 50 nm thickness, a silicon waveguide layer of 250 nm, and a silica substrate. The width of the biomolecular layer and the silicon waveguide is 500 nm for both. The effective refractive indices of the ssDNA- and

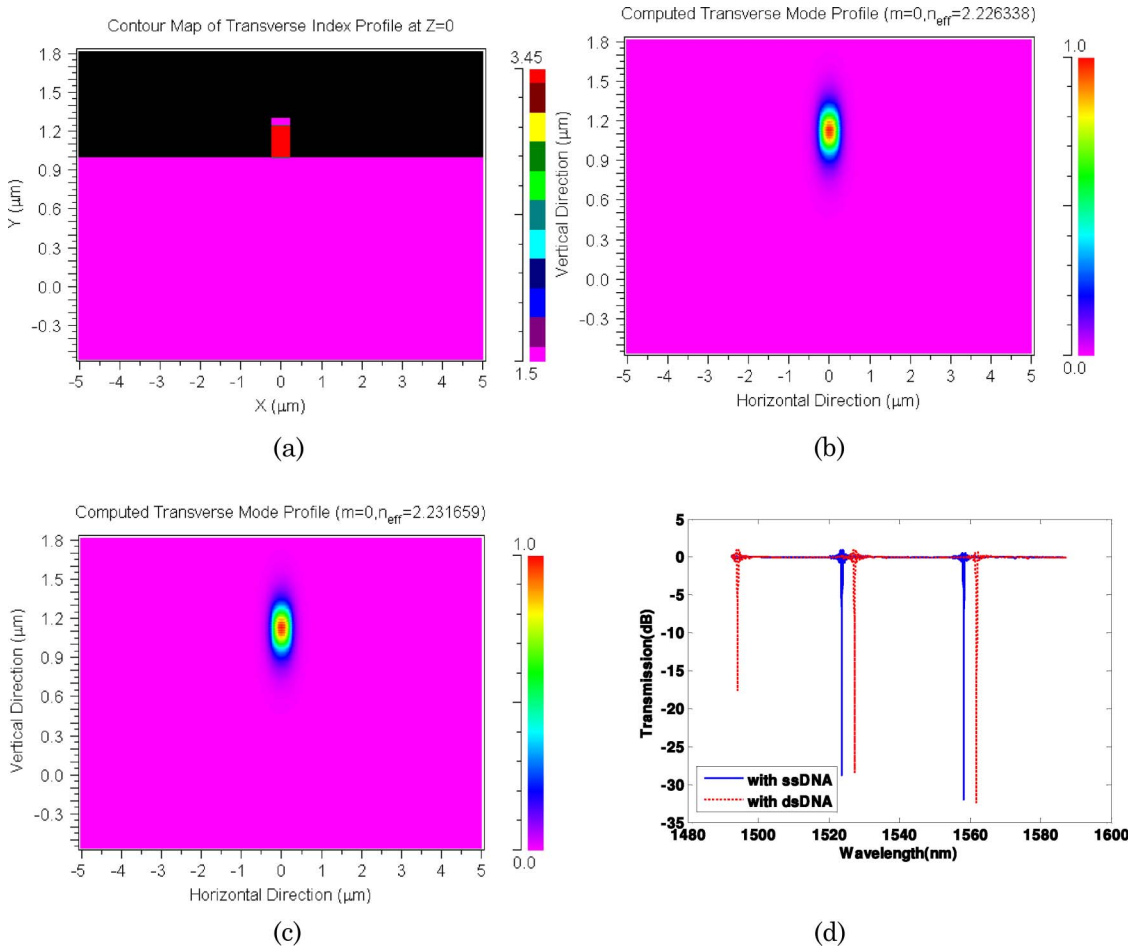

Fig. 2. (Color online) (a) 2D illustration of the multilayer structure. The electrical field profile of the fundamental TE mode propagating through the structure shown in (a) with (b) the ssDNA and (c) the dsDNA on the top layer. (d) Simulation results of transmission spectra before (solid curve) and after (dashed curve) detection in double concentric ring resonators with a 5 μm outer ring radius, 0.5 μm waveguide width, 0.3 μm waveguide–ring air gap, and 0.2 μm ring–ring air gap.

dsDNA-immobilized waveguides are 2.226338 and 2.231659, respectively. The effective indices are then used in the simulations of the transmission spectra before and after DNA molecular detection in the double-ring resonators.

After carefully optimizing the structural parameters, the transmission notch depth reaches –30 dB. Figure 2(d) shows the resonance shift during DNA detection. The resonance-wavelength shifts at wavelengths of 1523 and 1558 nm are 3.568 and 3.634 nm, respectively. For a detection area of 27.646 μm^2 at ~1558 nm, the bulk detection sensitivity is 683 nm RIU^{-1}. The sensitivity is much improved compared with the published result of 70 nm RIU^{-1} in [8]. Both the enhanced transmission notch depth and the enlarged detection area contribute to the improved sensitivity. With a larger detection area, more complementary molecules can be attracted by the probe, leading to a larger environmental change and resonance shift. Deeper notches also facilitate the detection process, since a small resonance shift will result in a significant change in the transmitted signal power.

B. Detection in the Ring–Ring Air Gap

As discussed in Section 2, mutual coupling between the rings plays a central role to achieve deep notch transmission spectra. It is therefore interesting to study the detection sensitivity when the probe is immobilized in the ring–ring air gap. We take the

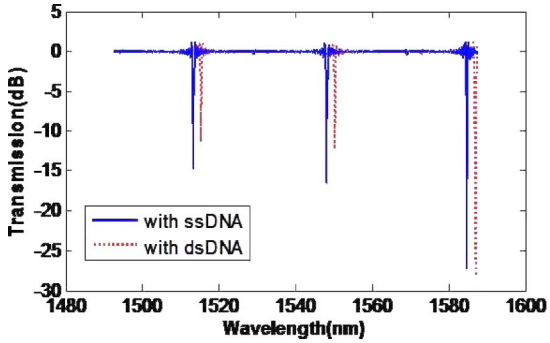

Fig. 3. (Color online) Simulation results of transmission spectra before (solid curve) and after (dashed curve) detection by double concentric ring resonators with a 5 μm outer ring radius when the probe is in the air gap.

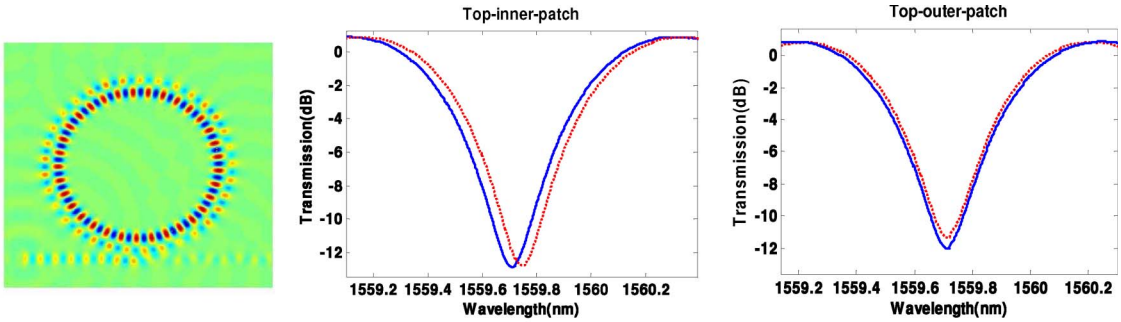

(a) (b) (c)

Fig. 4. (Color online) (a) Field distribution of the structure with 0.1 μm ring–ring and 0.1 μm waveguide–ring air gaps at the resonance wavelength of 1559.715 nm. Simulation results of transmission spectra before (solid curve) and after (dashed curve) patch detection on the top locations of the (b) inner and (c) outer ring resonators.

double-ring resonators with 0.2 μm ring–ring and 0.3 μm waveguide–ring air gaps. The total air-gap detection area is 5.53 μm^2. In Fig. 3 we observe that the resonance shifts around 1510, 1550, and 1580 nm in the transmission spectra are 1.91, 2.11, and 2.26 nm, respectively. The bulk refractive-index sensitivity is 396.616 nm RIU^{-1}. Thus, the double-ring structure functionalized on the silicon top is more attractive with a larger detection area and higher sensitivity compared with the detection method using the air gap.

4. Sensitivity Analysis

To study the detection sensitivity of the concentric microring resonators, we put a small dsDNA patch with a radius of 0.2 μm at different locations on top of the concentric ring resonators with the ssDNA top layer to observe the resonance shifts. We found that the shifts are dependent on the field distributions of the rings. The observed shift when the patch is put on the inner ring is different from that when the patch is added to the outer ring. The stronger the field is, the larger the shift is. However, on the same ring, regardless of the exact location of the patch, the induced shifts are the same.

For the resonant mode around 1559.7 nm, the field concentrates on the inner ring, as shown in Fig. 4(a). When the patch is put on the inner ring, a larger shift occurs, as evidenced in Fig. 4(b). On the other hand, a patch on the outer ring has only a slight effect on the resonance wavelength, as provided in Fig. 4(c). Figure 5(a) shows the opposite situation when the field exists mainly in the outer ring. The shift induced by the patch put on the outer ring [Fig. 5(c)] is larger than that on the inner ring [Fig. 5(b)].

The optical field at the resonance frequencies in Fig. 3 is similar to Fig. 5(a), which mainly concentrates on the outer ring. In this structure, the air gap between the rings is large and the mutual coupling is weak compared with the intrinsic loss of the inner ring. Therefore, there is only a slight field in the concentrically added ring. On the other hand, the ring–ring air gap in Fig. 4 is small and the mutual coupling is strong. For the outer ring, the intrinsic loss is increased by distributed coupling into the inner ring. For the inner ring, the distributed coupling dominates its intrinsic loss. Therefore the optical field concentrates on the inner ring. When the complementary DNA sequences happen to attach in the position where the maximum optical field exists, the perturbation is strongest and hence a large frequency shift will occur. If the refractive-index change occurs in the position close to the zero field distribution, the perturbation is weak and no noticeable frequency shift is induced. Because the sensitivity is related to the field distribution, it is more desirable to have an evenly distributed field in the

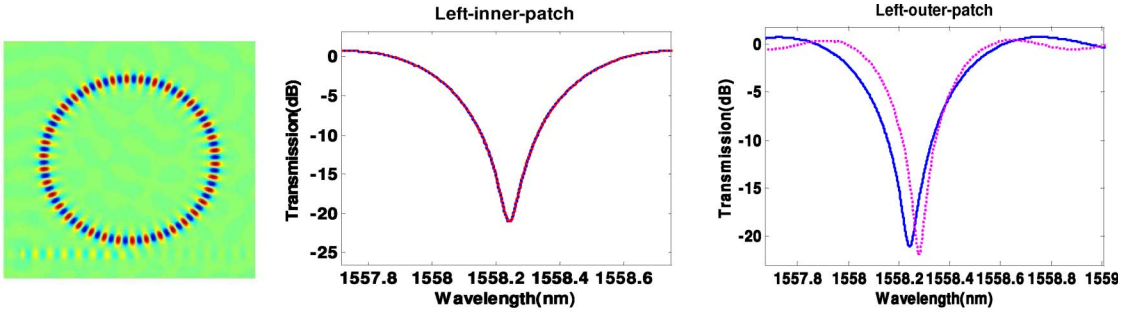

(a) (b) (c)

Fig. 5. (Color online) (a) Field distribution of the same structure as in Fig. 2(d) at the resonance wavelength of 1558.239 nm. Simulation results of transmission spectra before (solid curve) and after (dashed curve) patch detection on the top locations of the (b) inner and (c) outer ring resonators.

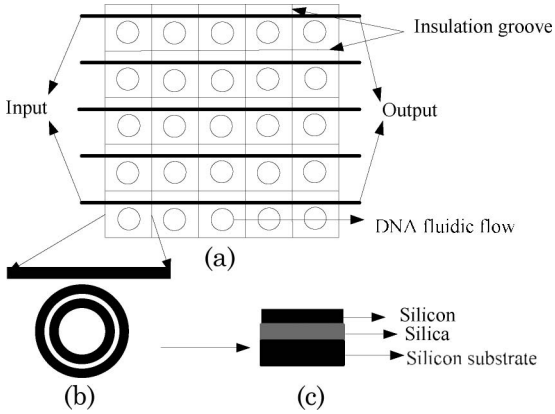

Fig. 6. (a) Schematic diagram of the compact parallel biosensor, (b) concentric microring resonators detection unit, (c) illustration of the SOI.

concentric ring resonators, which offer an enlarged detection area, constant sensitivity, and higher measurement accuracy.

From the formula $\lambda_{re} = \frac{n_{eff}\pi d}{m}$,one can see that the resonance wavelength λ_{re} is related to the effective refractive index n_{eff}. By a slight adjustment of their structural parameters, we can obtain ring-resonator units with different resonance wavelengths. When several different units are coupled to the same straight waveguide, their transmission spectra are independently and linearly superimposed [16]. Based on the former analysis, we propose an ultracompact, real-time, and label-free detection array as shown in Fig. 6.

Slightly tuned concentric microring resonator units with different resonance wavelengths are cascaded in a line along a straight waveguide and arranged in an array. When we pump the fluid flow to the sensing area, a resonance shift happens if the probe molecules attract their complementary molecules. From the transmission spectra at the output of a single waveguide one can get the molecular information of the fluid. We introduce the insulation groove to reduce the light interference from the adjacent units. If different probe molecules are immobilized on the top of the cascaded units, each resonant frequency in a FSR provides the information for its probes [16]. Thus this array can be used for parallel DNA detections.

5. Conclusion

Based on concentric microring resonators, we have proposed a sensitive, compact, label-free method to detect DNA hybridization. The detection sensitivities on top of the double concentric ring resonators and in the ring–ring air gap have been compared. The uniform sensitivity study shows that the field distribution affects the resonance shift.

This research was supported by the National Natural Science Foundation of China (NSFC), 60777040, Shanghai Rising Star Program Phase II, 07QH14008, the Interdisciplinary Fund of Biology and Engineering of Shanghai Jiao Tong University (SJTU), YG2007MS31, the Swedish Foundation for Strategic Research (SSF), and the Swedish Research Council (VR) .

References

1. O. Lazcka, F. J. Del Campo, and F. X. Munoz, "Pathogen detection: a perspective of traditional methods and biosensors," Biosens. Bioelectron. **22**, 1205–1217 (2007).
2. P. P. P. Debackere, S. Scheerlinck, P. Bienstman, and R. Baets, "Surface plasmon interferometer in silicon-on-insulator: novel concept for an integrated biosensor," Opt. Express **14**, 7063–7072 (2006).
3. A. Ymeti, J. Greve, P. V. Lambeck, T. Wink, S. W. F. M. van Hövell, T. A. M. Beumer, R. R. Wijn, R. G. Heideman, V. Subramaniam, and J. S. Kanger, "Fast, ultrasensitive virus detection using a Young interferometer sensor," Nano. Lett. **7**, 394–397 (2007).
4. Y. Li and L. Tong, "Mach—Zehnder interferometers assembled with optical microfibers or nanofibers," Opt. Lett. **33**, 303–305 (2008).
5. X. Guo and L. Tong, "Supported microfiber loops for optical sensing," Opt. Express **16**, 14429–14434 (2008).
6. A. Ksendzov and Y. Lin, "Integrated optics ring-resonator sensors for protein detection," Opt. Lett. **30**, 3344–3346 (2005).
7. A. Ksendzov, M. L. Homer, and A. M. Manfreda, "Integrated optics ring-resonator chemical sensor with polymer transduction layer," Electron. Lett. **40**, 63–65 (2004).
8. K. D. Vos, I. Bartolozzi, E. Schacht, P. Bienstman, and R. Baets, "Silicon-on-insulator microring resonator for sensitive and label-free biosensing," Opt. Express **15**, 7610–7615 (2007).
9. B. E. Little, S. T. Chu, H. A. Haus, J. Foresi, and J. P. Laine, "Microring resonator channel dropping filters," J. Lightwave Technol. **15**, 998–1005 (1997).
10. C. Manolatou, M. J. Khan, S. Fan, P. R. Villeneuve, H. A. Haus, and J. D. Joannopoulos, "Coupling of modes analysis of resonant channel add-drop filters," IEEE J. Quantum Electron. **35**, 1322–1331 (1999).
11. Z. Zhang, M. Dainese, L. Wosinski, and M. Qiu, "Resonance-splitting and enhanced notch depth in SOI ring resonators with mutual mode coupling," Opt. Express **16**, 4621–4630 (2008).
12. X. Li, Z. Zhang, Q. Yin, M. Qiu, and Y. Su, "Concentric silicon micro-ring resonators with enhanced transmission notch depth," in *Proceedings of the Asia– Pacific Optical Communications Conference (APOC)* (SPIE, 2008), 7135-25.
13. X. Li, Z. Zhang, Q. Li, M. Qiu, and Y. Su, "Label-free biosensor based on silicon-on-insulator concentric micro-ring resonators," in *Proceedings of the IEEE Photonics Global Conference* (IEEE, 2008).
14. S. Elhadj, G. Singh, and R. F. Saraf, "Optical properties of an immobilized DNA monolayer from 255 to 700 nm," Langmuir **20**, 5539–5543 (2004).
15. S. Mandal and D. Erickson, "Nanoscale optofluidic sensor arrays," Opt. Express **16**, 1623–1631 (2008).
16. X. Li, Z. Zhang, Q. Yin, M. Qiu, and Y. Su, "Ultra-compact parallel label-free biosensors based on concentric micro-ring resonators in silicon-on-insulator," in *Proceedings of the Asia Optical Fiber and Optoelectronic 2008 Exposition and Conference* (IEEE, 2008).